

This is the accepted manuscript made available via CHORUS. The article has been published as:

Coexistence of strong nematic and superconducting correlations in a two-dimensional Hubbard model

Shi-Quan Su and Thomas A. Maier

Phys. Rev. B **84**, 220506 — Published 22 December 2011

DOI: [10.1103/PhysRevB.84.220506](https://doi.org/10.1103/PhysRevB.84.220506)

Coexistence of strong nematic and superconducting correlations in a two-dimensional Hubbard model

Shi-Quan Su^{1,2,*}, and Thomas A. Maier¹

¹*Computer Science and Mathematics Division,
Center for Nanophase Materials Sciences,
Oak Ridge National Laboratory,
Oak Ridge, Tennessee 37831-6164, USA*

²*National Center for Computational Sciences,
Oak Ridge National Laboratory,
Oak Ridge, Tennessee 37831-6164, USA*
* shiquansu@hotmail.com

Using a dynamic cluster quantum Monte Carlo approximation, we study a two-dimensional Hubbard model with a small orthorhombic distortion in the nearest neighbor hopping integrals. We find a large nematic response in the low-frequency single-particle scattering rate which develops with decreasing temperature and doping as the pseudogap region is entered. At the same time, the d-wave superconducting gap function develops an s-wave component and its amplitude becomes anisotropic. The strength of the pairing correlations, however, is found to be unaffected by the strong anisotropy, indicating that d-wave superconductivity can coexist with strong nematicity in the system.

PACS numbers: 74.72.-h, 74.20.-z, 71.10.-w

Introduction- Nematic correlations, where the C_4 rotational symmetry of the square lattice is spontaneously broken and reduced to C_2 , have been observed in the electronic structure in a number of strongly correlated electron materials, including the strontium-ruthenate oxide compounds, the cuprates and the iron-pnictide materials¹. Despite the presence of very small structural anisotropies in the plane, these systems display very large nematic anisotropies in properties such as the dc and infrared resistivities², the magnetoresistance³, the Nernst signal⁴, the neutron scattering spectrum⁵ as well as in scanning tunneling spectroscopy^{6,7}.

From a theoretical perspective, the idea that the pseudogap in the cuprates may be associated with a nematic phase, which arises from melting of a stripe ordered phase, was first discussed in Ref.⁸ and later expanded on in Ref.⁹. A first microscopic theory of how a nematic phase can emerge from an isotropic Fermi liquid through a Fermi surface instability was presented in Ref.¹⁰. And indeed, both strong-coupling RVB slave-boson mean-field calculations for the 2D t-J model^{11,12} and weak-coupling functional renormalization group studies¹³⁻¹⁵ of the 2D Hubbard model have found a Pomeranchuk instability towards a d-wave Fermi surface deformation (for a review see Ref.¹⁶). This nematic instability has been found to compete with d-wave superconductivity, a picture that has also emerged from exact diagonalization¹⁷ and variational Monte Carlo studies¹⁸ of the t-J model.

Here we are interested in the question of how a small orthorhombic distortion that exists in the system affects the electronic structure in a strongly correlated electron system. Consistent with experiments, recent theoretical studies have found a large nematic response to a small

structural anisotropy. In particular, a recent study of the 2D Hubbard model using cellular dynamical mean-field theory and a dynamic cluster approximation (DCA) of a small 2×2 -site cluster has found a large nematic response in the low-frequency behavior of the single-particle self-energy as well as in the conductivity when the system is doped towards the Mott insulating state²². This study was restricted to zero temperature and a small 2×2 cluster. Here, using a larger 4×4 cluster DCA calculation of a similar 2D Hubbard model with a small anisotropy in the single-particle hopping integral, we study the temperature dependence of the nematic response as well as its connection with the pseudogap and its interplay with the superconducting behavior of this model.

We find a large nematic anisotropy in the single-particle scattering rate, which increases with decreasing temperature and doping. We show that this nematic anisotropy becomes significant inside the pseudogap region below a temperature $T^*(\delta)$, pointing to a deep relationship between the pseudogap and nematic correlations. Moreover, we find that the orthorhombicity in the single-particle hopping leads to an anisotropic superconducting gap, with both *d*-wave and *s*-wave components similar to what was discussed in Ref.⁸, but has no effect on the superconducting transition temperature.

Formalism- The orthorhombic 2D Hubbard model we analyze²²,

$$H = \sum_{\langle ij \rangle, \sigma} (t_{ij} - \mu \delta_{ij}) c_{i\sigma}^\dagger c_{j\sigma} + U \sum_i n_{i\uparrow} n_{i\downarrow} \quad (1)$$

has a nearest neighbor transfer integral $t_{ij} = -t_{x/y}$ for hopping along the *x*- and *y*-direction, respectively, a Coulomb repulsion *U* and chemical potential μ . As in

Ref.²², we use a small anisotropy $t_{x/y} = t(1 \pm \xi/2)$ with $\xi = 0.04$ to break the C_4 lattice symmetry of the model. In the following we will measure energies in units of t and set the Coulomb repulsion $U = 6t$ unless otherwise noted.

We will use the DCA to study the model in Eq. (1). The DCA^{19,20} maps the bulk lattice problem onto an effective periodic cluster embedded in a self-consistent dynamic mean-field that is designed to represent the remaining degrees of freedom. The DCA calculations were carried out on a 4×4 cluster and the effective cluster problem was solved using a Hirsch-Fye quantum Monte Carlo algorithm²¹.

Results- In contrast to the 2×2 -site cluster study performed in²², we have found that, in the 4×4 -site cluster, an additional next-nearest neighbor hopping t' reduces the nematic response relative to that found for $t' = 0$. We therefore set $t' = 0$ in the 4×4 -site cluster calculations.

In order to examine how the directional anisotropy in the hopping integral affects the Fermi surface of the correlated system, we plot in Fig. 1 the gradient of the momentum distribution function, $|\nabla n(\mathbf{k})|$ with $n(\mathbf{k}) = 2\langle c_{\mathbf{k}\sigma}^\dagger c_{\mathbf{k}\sigma} \rangle$, in the first quadrant of the Brillouin zone. We have interpolated the DCA cluster self-energy $\Sigma(\mathbf{K}, i\omega_n)$, which is defined on a 4×4 grid of \mathbf{K} -points using a smooth spline.

The panels on the left show the results for the 4×4 -site cluster for $U = 6t$ and $t' = 0$. Panels a) through c) show results for different dopings δ calculated at a fixed temperature $T = 0.074t$, while panel d) shows the result for a lower temperature $T = 0.05t$ and a doping of $\delta = 0.05$. From this one sees that at high temperatures and doping levels, $|\nabla n(\mathbf{k})|$ is fairly symmetric. But at low temperatures and dopings, directional anisotropy clearly develops in both its shape and, much more noticable, in its magnitude, with a larger value in the region near $(0, \pi)$ than near $(\pi, 0)$. As pointed out in Ref.²², this reflects a stronger anisotropy in the imaginary part of the self-energy than in the real part.

This result is supported by the plots of the real and imaginary parts of the self-energy in Fig. 2. There one clearly sees that the imaginary part exhibits qualitatively different behavior between $(\pi, 0)$ and $(0, \pi)$, while the real part shows much less anisotropic. For $\mathbf{K} = (0, \pi)$, $|\text{Im} \Sigma(\mathbf{K}, \omega_n)|$ displays Fermi liquid like behavior with a downturn at low frequencies, while for $\mathbf{K} = (\pi, 0)$, it keeps rising with decreasing ω_n . A similarly strong angle dependence of the self-energy in the nematic phase was also found in Ref.¹⁰. In addition, one sees that the anisotropy in the imaginary part goes away at high frequencies, consistent with the behavior found in Ref.²².

We generally find that the nematic response in the 4×4 -site cluster is not larger than that found in the 2×2 -site cluster. As an example, we show on the right hand

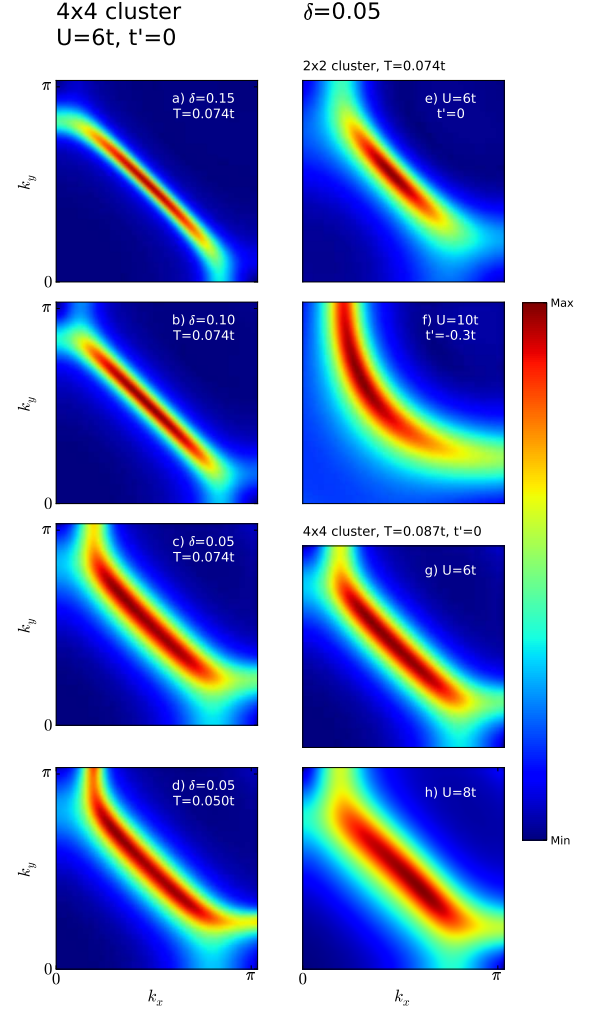


FIG. 1: (Color online) Plots of the gradient of the k-space occupation, $|\nabla n_k|$ in the first quadrant of the Brillouin zone, calculated for the system with small directional anisotropy. On the left, results are shown for the 4×4 cluster with $U = 6t$ and $t' = 0$ in panels a) through c) for a fixed temperature $T = 0.074t$ but varying doping as indicated, and in panel d) for a lower temperature $T = 0.05t$ and a doping $\delta = 0.05$. The right side illustrates the effects of cluster size and varying parameters for a doping $\delta = 0.05$. Panels e) and f) show results for a 2×2 cluster for different values of U and t' as indicated. Panels g) and f) show results for the 4×4 cluster for $t' = 0$ for different values of U .

side of Fig. 1 in panels e) and f) results for the 2×2 -site cluster for $U = 6t$ and $t' = 0$ and $U = 10t$ and $t' = -0.3t$, respectively. Here one sees that in the 4-site cluster, the nematic response is dramatically increased for larger values of U and a finite $t' = -0.3t$. In the 16-site cluster, however, this does not seem to be the case. While a systematic study of larger values of U and finite t' is not possible in the 16-site cluster, because of the QMC sign problem, we show as an example in panels g) and h) 16-

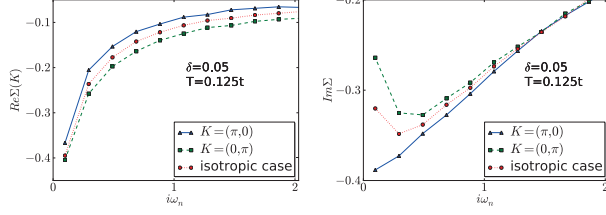


FIG. 2: (Color online) Real and imaginary parts of the self-energy $\Sigma(\mathbf{K}, \omega_n)$ versus frequency ω_n for $\mathbf{K} = (\pi, 0)$ and $(0, \pi)$ for a doping $\delta = 0.05$ and temperature $T = 0.125t$. Results for both the anisotropic and isotropic cases are shown.

site cluster results for two different values of U , $U = 6t$ and $8t$, respectively. There is no obvious enhancement of the response for the larger value of U .

In order to further examine the temperature and doping dependence of the nematic response, we have calculated the quasiparticle weight approximated by

$$Z_{\mathbf{K}} = \left[1 - \text{Im} \frac{\Sigma(\mathbf{K}, \pi T)}{\pi T} \right]^{-1}. \quad (2)$$

In Fig. 3 we plot the nematic anisotropy of $Z_{\mathbf{K}}$ defined as

$$\sigma_Z = \frac{Z_{(0,\pi)} - Z_{(\pi,0)}}{Z_{(0,\pi)} + Z_{(\pi,0)}} \quad (3)$$

for the 4×4 -site cluster. One clearly sees that the nematic response increases with decreasing temperature and doping, reaching remarkable levels of over 50% at the lowest temperature and doping level we have studied.

Also indicated in this plot by the solid blue line is the pseudogap temperature $T^*(\delta)$ as in ²³. Below this temperature, a pseudogap opens in the single-particle density of states as well as in the spin excitations. Here we have determined $T^*(\delta)$ from the temperature T at which the uniform magnetic susceptibility $\chi_s(\mathbf{q} = 0, T)$ has a maximum ²⁴. It is interesting to note that this temperature is not affected by the orthorhombic anisotropy in the Hamiltonian. Conversely, as evidenced by this plot, the emergence of a strong nematic response is intimately linked to the opening of the pseudogap. Outside the pseudogap region, the nematic anisotropy is small. With decreasing temperature and doping, it increases dramatically along the pseudogap temperature $T^*(\delta)$ and then saturates deep inside the pseudogap region. This points towards the pseudogap being a necessary precondition for nematic physics to appear in this system.

Finally, we note that we do not find spontaneous symmetry breaking to a nematic state in the C_4 symmetric model, i.e. for $\xi = 0$, for the temperatures we have studied. Note, however, that this does not exclude the possibility of an instability at a lower temperature. In fact, the large nematic response we find at the temperatures

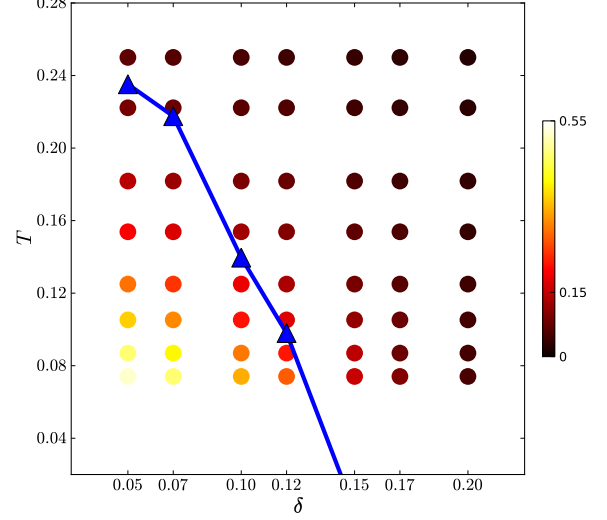


FIG. 3: (Color online) Color map of the anisotropic ratio of the quasiparticle weight, σ_Z , over the temperature-doping plane, for $U=6t$. The blue curve indicates the pseudogap temperature $T^*(\delta)$ which is obtained as the temperature at which the uniform magnetic susceptibility $\chi_m(\mathbf{q} = (0, 0), T)$ has a maximum.

we have studied is strongly suggestive of an instability at lower temperatures. A detailed study of this issue is beyond the scope of the present paper and will be the subject of future work.

It is interesting to ask how the strong nematic anisotropy that is present in the single-particle scattering rate affects the superconducting behavior of the system. In Ref.⁸ it was pointed out that, in a nematic phase, the superconducting order parameter will have mixed $d_{x^2-y^2}$ and extended s symmetry. This question was also addressed in a previous slave-boson mean-field study of an anisotropic t-J model in Ref.¹¹.

Here we study the superconducting behavior of the anisotropic Hubbard model (1) by solving the Bethe-Salpeter equation in the particle-particle channel

$$-\frac{T}{N} \sum_{K'} \Gamma^{pp}(K, K') \chi_0^{pp}(K') \phi_\alpha(K') = \lambda_\alpha \phi_\alpha(K), \quad (4)$$

where $K = (\mathbf{K}, \omega_n)$ and $\Gamma^{pp}(K, K')$ is the irreducible particle-particle vertex with center of mass momentum and frequency $Q = 0$. The coarse-grained bare particle-particle Green's function $\chi_0^{pp}(K) = N_c/N \sum_{\mathbf{k}} G_\uparrow(\mathbf{K}' + \mathbf{k}', \omega_n) G_\downarrow(-\mathbf{K} - \mathbf{k}, -\omega_n)$ is calculated from the lattice Green's function $G_\sigma(\mathbf{k}, \omega_n) = [i\omega_n - \epsilon_{\mathbf{k}} + \mu - \Sigma(\mathbf{K}, \omega_n)]^{-1}$. The system undergoes a superconducting transition at the temperature T_c where the leading eigenvalue λ_α becomes one, and the momentum and frequency dependence of the corresponding eigenvector $\phi_\alpha(K)$ determines the symmetry of the superconducting state. At T_c , $\phi_\alpha(K)$ becomes identical to the superconducting gap

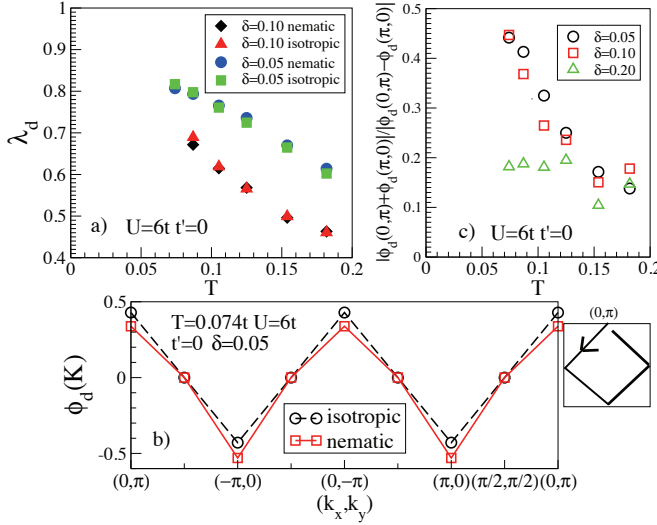


FIG. 4: (Color online) (a) Leading d-wave eigenvalues λ_d of the Bethe-Salpeter equation (4) in the particle-particle channel versus temperature. The eigenvalues for both the isotropic and anisotropic models are plotted. (b) The momentum dependence of the leading eigenvector $\phi_d(K, \pi T)$ at the lowest Matsubara frequency along the path in Brillouin zone shown in the inset. (c) The relative s-wave contribution to the d-wave contribution, $|\phi_d(\pi, 0) + \phi_d(0, \pi)| / |\phi_d(\pi, 0) - \phi_d(0, \pi)|$, as a function of temperature for different dopings.

function. In the isotropic model, the instability occurs in the spin singlet, even frequency channel and the leading eigenvector has *d*-wave symmetry²⁵. Here we focus on the low-doping region, where the nematic response of the anisotropic model is most pronounced.

Fig. 4a shows the temperature dependence of the leading eigenvalues of the anisotropic and isotropic models for two different dopings $\delta = 0.10$ and 0.05 . In the temperature range we could access — the QMC Fermion sign problem prevents us from going to lower temperatures — the leading eigenvalues of the isotropic ($\xi = 0$) and anisotropic ($\xi = 0.04$) models are essentially identical. This indicates that the strong nematic anisotropy which is present in the single-particle scattering rate has essentially no effect on the strength of the pairing correlations. We also calculated the leading eigenvalue in an 8-site cluster, which allows us to reach the temperature where the eigenvalue crosses one. There we find that the superconducting transition temperature T_c of the anisotropic model is unchanged from the isotropic case.

In Fig. 4b we plot the momentum dependence of the leading eigenvector $\phi(\mathbf{K}, \pi T)$ along the line indicated in the inset. From this one sees that in the anisotropic case, it has predominantly *d*-wave structure, just as in the isotropic model. There is an additional *s*-wave contribution in the anisotropic model, which causes an anisotropy between $(\pi, 0)$ and $(0, \pi)$, but leaves the nodal point unchanged.

In Fig. 4c, we plot the *s*-wave contribution related to *d*-wave $|\phi((\pi, 0), \pi T) + \phi((0, \pi), \pi T)| / |\phi((\pi, 0), \pi T) - \phi((0, \pi), \pi T)|$ as a function of temperature for different dopings. Once again, we find that the anisotropy in the eigenvector develops and increases when the system is cooled and doped into the pseudogap region.

These results demonstrate that superconductivity can coexist with nematicity in the system. In addition, they indicate that the strength of the pairing correlations and T_c are essentially unaffected by the large anisotropy present in the single-particle scattering rate. This is similar to what was found in earlier slave-boson mean-field calculations¹¹.

Conclusions We have used a dynamic cluster quantum Monte Carlo approximation to study a two-dimensional Hubbard model with a small (4%) orthorhombic distortion in the nearest-neighbor hopping integrals $t_x \neq t_y$. We have found a large nematic response, i.e. a difference in the electronic properties between $\mathbf{K} = (\pi, 0)$ and $(0, \pi)$, with levels up to 55% in the scattering rate $\text{Im} \Sigma(\mathbf{K}, \omega_n)$, which develops as one enters the pseudogap phase and increases as the doping and temperature is further reduced. Similar behavior is found in the *d*-wave superconducting gap function, which develops an *s*-wave component in the pseudogap phase which reaches levels up to 40%. In contrast, we find that the strength of the pairing correlations is essentially unaffected by these anisotropies. These results demonstrate a close link between the pseudogap and nematic correlations, and indicate that *d*-wave superconductivity can coexist with a strong nematicity in the system.

Acknowledgments We would like to thank S. Okamoto and D.J. Scalapino for helpful discussion. Shi-Quan Su performed the above research under contract number DE-AC05-00OR22750 between the U.S. Department of Energy and Oak Ridge Associated Universities. A portion of this research was conducted at the Center for Nanophase Materials Sciences, which is sponsored at Oak Ridge National Laboratory by the Office of Basic Energy Sciences, U.S. Department of Energy. This research used resources of the Oak Ridge Leadership Computing Facility at Oak Ridge National Laboratory, which is supported by the Office of Science of the U.S. Department of Energy under Contract No. DE-AC05-00OR22725.

-
- ¹ E. Fradkin, et al., *Annu. Rev. Condens. Matter Phys.* **1**, 153 (2010).
- ² Y. Ando, K. Segawa, S. Komiya, A. N. Lavrov, *Phys. Rev. Lett.* **88**, 137005 (2002).
- ³ R. A. Borzi, et al., *science*, **315**, 214 (2007).
- ⁴ R. Daou, et al., *nature*, **463**, 519 (2010).
- ⁵ V. Hinkov, et al., *science*, **319**, 597 (2008).
- ⁶ S. A. Kivelson, et al. *Rev. Mod. Phys.* **75**, 1201 (2003).
- ⁷ M. J. Lawler, et al., *Nature*, **466**, 347 (2010).
- ⁸ V. Emery et al., *Phys. Rev. B* **56**, 6120 (1997).
- ⁹ S. A. Kivelson et al., *Nature* **393**, 550 (1998).
- ¹⁰ V. Oganesyan et al., *Phys. Rev. B* **64**, 195109, (2001).
- ¹¹ H. Yamase and H. Kohno, *J. Phys. Soc. Jpn.*, **69**, 2151 (2000).
- ¹² H. Yamase and W. Metzner, *Phys. Rev. B*, **73**, 214517 (2006).
- ¹³ C. J. Halboth and W. Metzner, *Phys. Rev. Lett.*, **85**, 5162 (2000).
- ¹⁴ I. Grote, E. K rding, and F. Wegner, **126**, 13854 (2002).
- ¹⁵ A. Neumayr and W. Metzner, *Phys. Rev. B*, **67** 035112, (2003).
- ¹⁶ M. Vojta, *Adv. in Phys.*, **58**, 699, (2009).
- ¹⁷ A. Miyanaga and H. Yamase, *Phys. Rev. B*, **73** 174513 (2006).
- ¹⁸ B. Edegger, V. N. Muthukumar, and C. Gros, *Phys. Rev. B*, **74**, 165109 (2006).
- ¹⁹ M. H. Hettler, et al., *Phys. Rev. B* **58**, R7475 (1998); M. H. Hettler, et al., *Phys. Rev. B* **61**, 12739 (2000).
- ²⁰ T. Maier, M. Jarrell, T. Pruschke, and M. H. Hettler, *Rev. Mod. Phys.* **77**, 1027 (2005).
- ²¹ M. Jarrell, T. Maier, C. Huscroft, and S. Moukouri, *Phys. Rev. B*, **64**, 195130, (2001).
- ²² S. Okamoto, D. Senechal, M. Civelli, and A. -M. S. Tremblay, *Phys. Rev. B* **82**, 180511(R) (2010).
- ²³ S. -X. Yang et al., *Phys. Rev. Lett.* **106**, 047004 (2011).
- ²⁴ S. -Q. Su, et al., *Phys. Rev. A* **81**, 051604(R) (2010), S. -Q. Su, et al., *Phys. Rev. B* **80**, 104517 (2009).
- ²⁵ T. Maier, M. Jarrell, and D. Scalapino, *Phys. Rev. Lett.*, **96**, 047005 (2006).